PCCP

Accepted Manuscript

ROYAL SOCIETY OF CHEMISTRY

www.rsc.org/pccp

Charge-switchable gold nanoparticles for enhanced enzymatic thermostability

Shiv Shankar,[a] Sarvesh K. Soni,[b] Hemant K. Daima,[a,b,c] PR. Selvakannan,[b] Jayant M. Khire,[d] Suresh K. Bhargava,[b,*] Vipul Bansal[a,*]

[a]Ian Potter NanoBiosening Facility, NanoBiotechnology Research Laboratory (NBRL), School of Applied Sciences, RMIT University, GPO Box 2476V, Melbourne, VIC 3001, Australia

[b]Center for Advanced Materials and Industrial Chemistry (CAMIC), School of Applied Sciences, RMIT University, GPO Box 2476V, Melbourne, VIC 3001, Australia

[c]Nano-Bio Interfacial Research Laboratory (NBIRL), Department of Biotechnology, Siddaganga Institute of Technology, Tumkur 572103, Karnataka, India

[d]National Collection of Industrial Microorganisms, National Chemical Laboratory, Pune 411008, Maharashtra, India

*Corresponding Author: Tel: +61 3 99252121; Fax: +61 3 99253747;

E-mail (V.B.): vipul.bansal@rmit.edu.au; E-mail (S.K.B.): suresh.bhargava@rmit.edu.au

Abstract

This study illustrates a facile strategy for efficient immobiolisation of enzymes on metal nanoparticle surface. The strategy proposed here enables enzymatic activity to be retained while increasing the enzyme thermostability. It is demonstrated that the use of a zwitterionic amino acid tyrosine as a reducing and capping agent to synthesise gold nanoparticles allows efficient immobilization of phytase enzyme through charge-switchable electrostatic interactions. The detailed kinetic and thermodynamic studies reveal that the proposed enzyme immobilization strategy improves the overall quality of phytase by reducing the activation energy required for substrate hydrolysis and broadening the temperature window in which immobilized enzyme is able to operate. The outcomes of this study indicate that the underlying zwitterionic nature of 20 natural amino acids along with significant variability in their isoelectric points and hydropathy indices as well the ability of some of the amino acids to reduce metal ions is likely to offer significant opportunities for tailoring nano-bio interfaces in a rational manner for a range of biological applications.

Keywords. Gold nanoparticle; tyrosine; phytase; immobilization; activation energy

1. Introduction

Phytic acid (myo-inositol hexakisphosphate) is a major storage form of phosphorus in cereals and legumes, representing 18-88 % of total phosphorus content.[1] Phytase group of enzymes (EC 3.1.3.8 and EC 3.1.3.26) belong to the family of histidine acid phosphatases that have the capability to catalytically degrade phytic acid and its salt (phytate) to yield biomedically important products such as inositol, inositol monophosphate, myo-inositol phosphates and inorganic phosphate.[2] Phytase has additional applications as an animal feed additive, as a soil amendment agent and for the semi-synthesis of peroxidases.[3] Due to the ongoing environmental concerns related to undigested phosphorus released by animal livestock, and the outstanding ability of this enzyme to liberate phosphorus from a variety of substrates, Phy A, an enzyme produced by *Aspergillus niger*, has been globally adopted as an animal feed additive.[4] Although recent market trends have clearly shown phytase to be an important enzyme, the feedstock processing conditions require improved thermostability of this enzyme to attain wider adaptability for industrial applications.[5] Various strategies are employed to improve the thermostability of enzymes including the use of additives, introduction of disulfide bonds, site-specific mutagenesis, and chemical modifications.[6-10] However, in all these cases, the recovery of the water-soluble enzyme to allow enzyme reusability remains challenging.[11] Therefore, an alternative strategy involving enzyme immobilization on to water-insoluble solid supports has been extensively adopted to facilitate product and enzyme separation, as well as enzyme recovery.[12] Enzyme immobilization on solid supports can although be achieved by a variety of methods such as entrapment, ionic interaction, covalent attachment, encapsulation and adsorption onto hydrophobic or hydrophilic surfaces, each of these methods have their own pros

and cons, as some methods allow high enzyme loading while others allow optimal thermostability.[12-14]

In the specific contest of phytase immobilization, enzyme supports explored so far include synthetic allophane, natural montmorillonite and spores of *Bacillus polyfermenticus*.[14,15] Conversely, the use of nanoparticles as an enzyme support is advantageous as their extremely high surface to volume ratio allows large amount of enzyme loading without causing significant stearic hindrance during the enzymatic reaction, with an option of facile enzyme recovery.[16] We previously demonstrated that under appropriate conditions, phytase molecules can self-assemble in ionic liquids to form catalytically-active enzyme nanocapsules that allow phytase reusability; however, these self-assembled systems failed to increase the enzyme thermostability.[17,18] It is also noteworthy that most of the previous enzyme immobilisation studies, including our previous work, have predominantly focussed on studying the nature of enzyme binding on nanoparticle surface, without necessarily focussing on influence of nanoparticle surface on the enzyme kinetic and thermodynamic parameters, except for the relatively few studies.[19,20] Moreover, different strategies adopted for enzyme immobilisation on the nanoparticle surface typically require nanoparticle surface modification using organic ligands, which is not ideal, as such ligands may interfere with enzymatic reactions.[21] We recently demonstrated that natural amino acids such as tyrosine can be employed as unique reducing agents for the synthesis of charge-switchable metal nanoparticles.[22,23] The zwitterionic nature of amino acid molecules present on the surface of these bio-tailorable metal nanoparticles allows these materials to show a pH-dependent charge-switchable property. This unique property of amino acids provides a facile handle to control the nanosurface chemistry to facilitate the binding of a variety of molecules through electrostatic interactions.[24,25] In our recent work, the control of nanoparticle surface corona through this

strategy allowed us to efficiently bind bulky clusters of polyoxometalates on the surface of tyrosine-reduced Au and Ag nanoparticles, which provided bacterial targeting attributes to these nanomaterials without causing toxicity to mammalian cells.[22,23] Further, the charge-switchability of these amino-acid (tyrosine or tryptophan) capped metal nanoparticles allowed selective binding to analyte molecules, leading to surface enhanced Raman scattering (SERS) applications.[26]

In the current study, we demonstrate that this strategy can be extended to employ tyrosine-capped gold nanoparticles ($AuNPs^{Tyr}$) for efficient immobilisation of phytase enzyme through electrostatic interactions. We have chosen gold as the enzyme support due to its well-established high biocompatibility.[27] We further compare the temperature-dependent enzymatic activity of immobilized phytase ($AuNPs^{Tyr}$/Phytase) with native phytase to elucidate the influence of enzyme immobilization on its thermostability, kinetics and thermodynamics. The immobilized phytase was also investigated for its ability to retain enzymatic activity during repeated cycles. To the best of the authors' knowledge, this is the first report on the utilization of amino acid-functionalized AuNPs for phytase immobilization that leads to increased thermostability and usability of this industrially important enzyme.

2. Materials and methods

2.1. Chemicals and reagents

Tetrachloroauric acid ($HAuCl_4$), L-tyrosine, potassium hydroxide (KOH), phytic acid sodium salt and dialysis tubing cellulose membrane were purchased from Sigma-Aldrich, U.S.A. All the solutions were prepared using deionized MilliQ water. All the chemicals used were of analytical grade and used as received, unless specified.

2.2. *Phytase assay and protein estimation*

Phytase I was purified from *A. niger* as described previously and enzyme activity was measured as described earlier with minor modifications.[28,29] Briefly, the reaction of phytase with phytic acid was carried out at pH 2.5 (100 mM Glycine-HCl buffer) at 55 °C for 30 min and the liberated inorganic phosphate was measured by a modification of the ammonium molybdate method.[30] A freshly prepared 4 mL solution of acetone : 5 N H_2SO_4 : 10 mM ammonium molybdate (2:1:1 v/v/v), followed by 400 µL of 1 M citric acid was added to the assay mixture and absorbance was measured at 370 nm. The phytase activity was expressed as the amount of phosphorus release (in M) by 1 M of enzyme per second under standard assay conditions. Each experiment was carried out in triplicates, and the values reported are the mean of three independent experiments in which a maximum of 5% variability was observed. The enzyme concentration was determined by Bradford assay, using bovine serum albumin (BSA) as a standard.[31]

2.3. *Synthesis of tyrosine-functionalized gold nanoparticles ($AuNPs^{Tyr}$)*

$AuNPs^{Tyr}$ were synthesized by boiling 400 mL aqueous solution consisting of 0.1 mM L-tyrosine and 1 mM KOH followed by the addition of the aqueous solution of $HAuCl_4$ to the final concentration of 0.2 mM. This ruby-red $AuNPs^{Tyr}$ solution was concentrated to 20 mL by further boiling followed by dialysis in deionized water (three hours and subsequently overnight) using processed cellulose dialysis membrane to remove the potentially excess KOH, unreduced $AuCl_4^-$ ions and unbound tyrosine molecules. The concentration of $AuNPs^{Tyr}$ was determined by atomic absorption spectrophotometer (AAS) after digesting nanoparticles with aqua regia, revealing the Au equivalent concentration of 780 µg/mL (780 ppm) in the $AuNPs^{Tyr}$ stock solution.

2.4. *Immobilization of phytase on $AuNPs^{Tyr}$ to form $AuNPs^{Tyr}$/Phytase nanozyme-composite*

Different amounts of AuNPs^{Tyr} (0.5 mL) were incubated with 0.5 mL of 1 µg (0.004 nM) native phytase in 10 mM Gly-HCl buffer (pH 2.5), leading to final AuNPs^{Tyr} concentration of 78, 156, 234, 312 and 390 µg/mL (Table S1, supporting information). The binding of phytase to AuNPs^{Tyr} surface was achieved by incubating the reaction mixture at 25 °C for 2 h. The mixtures were centrifuged at 14,000 rpm for 30 min, and the supernatant was checked for the amount of phytase that remains unbound to AuNPs^{Tyr}. To achieve this, the AuNPs^{Tyr}/Phytase nanozyme-composite pellets were washed twice with 10 mM Gly-HCl buffer (pH 2.5) to remove potentially unbound phytase, if any, followed by pooling all the supernatants and determining the free phytase in the supernatant after creating the standard curves from native phytase. The same supernatants were also used to evaluate the phytase activity from unbound phytase, whereas, the activity of phytase in AuNPs^{Tyr}/Phytase pellets was evaluated by re-suspending the pellets in 1 mL of the same buffer and checking activity using ammonium molybdate phytase assay. The equivalent concentration of pristine AuNPs^{Tyr} and pristine phytase in buffer served as controls.

2.5. Physical characterization of AuNPs^{Tyr} and AuNPs^{Tyr}/Phytase

All the nanomaterials prepared in this study were characterized by UV-visible (UV-vis) spectroscopy using Varian Cary 50 spectrophotometer operated at a resolution of 2 nm; transmission electron microscopy (TEM) using JEOL 1010 instrument; dynamic light scattering (DLS) using ALV Fast DLS particle sizing spectrometer and zeta potential measurements using Malvern 2000 Zetasizer.

2.6. Biochemical characterization of native phytase and AuNPs^{Tyr}/Phytase nanocomposite

Optimum temperature of native phytase and AuNPs^{Tyr}/Phytase was investigated in the temperature range of 45-60 °C at pH 2.5. Temperature stability was determined by incubating pristine phytase and AuNPs^{Tyr}/Phytase at 65 °C for up to 2 h and 70 °C for up to 10 min.

Residual activity was expressed as a percentage by taking the initial activity as 100 %. For reusability studies, AuNPs^{Tyr}/Phytase was incubated with phytic acid at 55 °C for 5 min followed by centrifugation at 15,000 rpm (25,000 x g using Sorvall Benchtop Centrifuge with 30 x 2 mL fixed angle rotor) for 10 min to recover AuNPs^{Tyr}/Phytase, washing with buffer, and thereafter using for the next cycle.

2.7. Substrate kinetic and thermodynamic studies

Substrate kinetic and thermodynamic studies of native phytase and AuNPs^{Tyr}/Phytase were determined using previously reported methods.[32,33] Michaelis constant (*Km*) and maximal velocity (*Vmax*) of free phytase and AuNPs^{Tyr}/Phytase were determined by Michaelis–Menten method at 35-60 °C range while varying the substrate concentrations at different temperatures. *Vmax* is expressed as M of product formed per sec, and the turnover number (*Kcat*) is expressed as *Vmax* per M of active site (in present case phytase is tetramer of 66 kDa of each subunit). The energy of activation (*Ea*) of native phytase and AuNPs^{Tyr}/phytase was calculated from the slope of the linear representation of the plot of ln *Vmax* vs. $1/T$ from Arrhenius equation as $Ea = -\text{slope} \times R$ (where, R is the gas constant = 8.314 $JK^{-1}mol^{-1}$). Gibbs free energy (ΔG^*) was calculated by using the equation, $\Delta G = RT.\ln Kd$, where the values of *Km* were used for the dissociation constant *Kd*. Enthalpy (ΔH^*) was calculated from the equation $\Delta H = Ea - RT$, and entropy (ΔS^*) was calculated from the equation $\Delta S = (\Delta H - \Delta G)/T$, where T is the temperature in Kelvin. All experiments were performed in triplicates and the means of the experiments were considered for further calculations.

3. Results and discussion

Scheme 1 illustrates the different steps involved in the synthesis of $AuNPs^{Tyr}$/Phytase nanozyme-composite. Initially, tyrosine molecules are used to reduce $AuCl_4^-$ ions under alkaline conditions to form tyrosine-capped $AuNPs^{Tyr}$. Under alkaline conditions, phenolic group of tyrosine acts as a reducing functional group,[23] which assists in reduction of $AuCl_4^-$ ions to form $AuNPs^{Tyr}$, and during this process oxidized tyrosine molecules act as capping agent to stabilize $AuNPs^{Tyr}$ in the aqueous solution through its amine group.[22,26] The pH of the extensively dialyzed $AuNPs^{Tyr}$ solution was found to be 8.4, which is well above the isoelectric point of tyrosine (pI~5.66). Therefore, $AuNPs^{Tyr}$ should bear a negative surface charge at this pH, which was confirmed by the zeta potential value of -29 mV. In the next step, when equal volumes of $AuNPs^{Tyr}$ (pH 8.4) and phytase (in pH 2.5 Gly-HCl buffer) were mixed, the pH of these solutions dropped to 4.6. Since this solution pH is below the pI of tyrosine, at this solution pH, the zwitterionic nature of the surface-bound tyrosine molecules would have resulted in switching the surface of $AuNPs^{Tyr}$ to be positively charged. This was confirmed by obtaining the zeta-potential value of $AuNPs^{Tyr}$ in Gly-HCl buffer in the absence of phytase, which corresponded to +19.3 mV. Considering that the pI of phytase I used in this study is 3.65, phytase is expected to bear an overall negative charge at the solution pH of 4.6.[34] Therefore, under the experimental conditions employed in this study, negatively charged phytase molecules can electrostatically interact with positively charged $AuNPs^{Tyr}$, leading to the formation of $AuNPs^{Tyr}$/Phytase nanozyme-composites. It is also worth noting that phytase belongs to the class of histidine acid peroxidase (HAP) enzymes that are rich in histidine residues.[35] The high affinity of histidine to the metal surfaces is well-known,[19,20] and this ability of histidine is regularly employed to purify recombinant proteins using nickel columns, as these recombinant proteins are designed to express histidine residues on protein's C-terminal.[36] Therefore, the histidine-rich nature of

phytase is likely to further promote the strong binding of phytase to the $AuNPs^{Tyr}$ surface, leading to highly stable $AuNPs^{Tyr}$/Phytase nanozyme-composites. This strong non-covalent binding of phytase on $AuNPs^{Tyr}$ surface is particularly important, as covalent immobilization of enzymes on the nanomaterial surface has been observed to cause significant reduction in the enzymatic activity.[37]

Figure 1A further illustrates the optical images of $AuNPs^{Tyr}$ under different conditions, revealing that the pristine $AuNPs^{Tyr}$ in water are of ruby red color, indicative of good stability without showing any signs of aggregation. This high stability of pristine $AuNPs^{Tyr}$ is due to a strong surface coating of tyrosine molecules that also act as a capping agent during reduction of $AuCl_4^-$ ions. The negative surface charge of tyrosine molecules promotes electrostatic repulsion between $AuNPs^{Tyr}$ in water, leading to high stability. However, the stability of pristine $AuNPs^{Tyr}$ in Gly-HCl buffer is slightly compromised (purple solution) as the tyrosine molecules present on the surface of $AuNPs^{Tyr}$ may undergo ligand exchange with the high concentration (10 mM) of glycine amino acid present in the buffer. In contrast, as illustrated in Scheme 1, $AuNPs^{Tyr}$/Phytase nanozyme-composite was found to be stable (ruby red solution) in the Gly-HCl buffer due to the presence of bulky enzyme molecules (phytase) on the surface of these nanoparticles that are difficult to be replaced by significantly smaller glycine molecules in the solution.

The stability of different nanoparticle solutions is further evident from the respective UV-Vis absorbance spectra shown in Figure 1A. Pristine $AuNPs^{Tyr}$ solution shows a sharp surface plasmon resonance (SPR) feature with A_{max} at 522 nm that is characteristic of monodisperse spherical AuNPs,[38] whereas, the Au SPR shifts to 541 nm without any significant peak broadening in the case of $AuNPs^{Tyr}$/Phytase due to the change in local dielectric environment.[39]

Additionally, a shoulder feature at 260-280 nm was observed in the UV-Vis spectrum of $AuNPs^{Tyr}$ due to π-π* molecular transitions resulting from tyrosine-capping of $AuNPs^{Tyr}$, which becomes more pronounced in the case of $AuNPs^{Tyr}$/Phytase spectrum, further supporting the binding of phytase to $AuNPs^{Tyr}$ surface in the nanozyme-composite. Conversely, on exposure of $AuNPs^{Tyr}$ to Gly-HCl buffer, a significant broadening of the SPR feature along with a shift in absorbance maximum to 554 nm due to nanoparticle aggregation is observed, which is responsible for the change of solution color from ruby red to purple. The TEM image clearly shows that the pristine $AuNPs^{Tyr}$ in the water remain well-segregated quasi-spherical particles of monodispersity better than 85% and an average diameter of 6 nm with a standard deviation of 0.85 (Figure 1B). However, these $AuNPs^{Tyr}$ showed significant aggregation in 10 mM Gly-HCl buffer at pH 2.5 (TEM image not shown for brevity). Conversely, when phytase was pre-mixed in the buffer prior to the addition of $AuNPs^{Tyr}$ to form $AuNPs^{Tyr}$/Phytase, neither any significant nanoparticle aggregation, nor change in nanoparticle morphology or size was observed (Figure 1C). Further, DLS spectroscopy measurements revealed that the pristine $AuNPs^{Tyr}$ had an average hydrodynamic radius of 14.8 nm, which increased to 38.6 nm in the case of $AuNPs^{Tyr}$/Phytase nanozyme composite due to phytase immobilization. Since DLS provides information about the hydrodynamic radii of particles in solution, an apparent increase in $AuNPs^{Tyr}$ size from DLS over TEM measurements post-phytase functionalization further indicates successful biofunctionalization of $AuNPs^{Tyr}$ with phytase. The outcomes of these physico-chemical characterization experiments show the potential of zwitterionic amino acids such as tyrosine to form biologically stable $AuNPs^{Tyr}$ that can act as good support for controllable enzyme immobilization.

Further, binding efficiency of phytase on the surface of $AuNPs^{Tyr}$ and the ability of these nanoparticles to retain the enzyme activity after phytase binding was determined as a function of gold concentration while keeping phytase concentration constant. **Figure 2** shows that the immobilization yield of phytase progressively increases with the increase in $AuNPs^{Tyr}$ concentration, wherein an optimal $AuNPs^{Tyr}$ concentration is critical to achieving the highest activity yield in $AuNPs^{Tyr}$/Phytase nanozyme-composites. For instance, although 100% immobilization yield (binding) of phytase is observed at 390 ppm Au concentration, this nanocomposite could retain only 92% activity; whereas at 234 ppm Au concentration, even 96% of phytase binding is capable of retaining 95% activity yield (enzymatic activity) of the original phytase used. Therefore, further enzyme kinetic and thermodynamic studies were focussed on $AuNPs^{Tyr}$/Phytase nanozyme-composites containing 234 ppm equivalent of Au and 0.96 μg of phytase.

Investigation of the biochemical properties of $AuNPs^{Tyr}$/Phytase nanozyme composite at the known optimum pH for the native phytase activity (pH 2.5) revealed that after immobilization of phytase on AuNPs, although the optimum temperature for phytase activity did not change, the temperature stability of the enzyme increased significantly (**Figure 3**). While the optimum temperature of both the native and the immobilized phytase were remained at 55 °C, the relative activity of phytase at 65 °C increased to 73% after immobilization in contrast to 45% in the case of native phytase (Figure 3A). A time course comparison of residual enzyme activities at 65 °C further demonstrates that over 1 hour, the $AuNPs^{Tyr}$/Phytase nanozyme composite is able to retain 68% activity in contrast to native phytase that could retain only 52% enzyme activity (Figure 3B). When the half-lives of native and immobilized phytases are compared at a further higher temperature of 70 °C, the half-life of the enzyme is observed to increase by almost 100%

post-immobilization on AuNPs^{Tyr} surface (Figure 3C). These results clearly show that the immobilization of phytase in the form of AuNPs^{Tyr}/Phytase nanozyme composite significantly enhances the thermostability of this enzyme. This enhanced thermostability most likely arises from strong association of phytase with AuNPs^{Tyr} through electrostatic and histidine-metal interactions, which provides conformational rigidity to the phytase enzyme.[40]

Further, the influence of proposed immobilization strategy on change in enzyme kinetic and thermodynamic parameters was studied by determining the activities of native phytase and AuNPs^{Tyr}/Phytase nanozyme composite at different temperatures while varying the concentration of phytic acid substrate. The kinetic and thermodynamic parameters derived from the Lineweaver-Burk double reciprocal plots of native and immobilized phytase at different temperatures are summarized in **Table 1**. At all the tested temperatures in 35-50 °C range, the *Michaelis* constant (*Km*) of the immobilized phytase increased by 28-52% over that of native phytase. The increase in the *Km* was highest (236.8%) at the optimum temperature of 55 °C, wherein the apparent *Km* of native and immobilized phytase was found to be 0.76 x 10^{-3} and 2.56 x 10^{-3} M, respectively. Since *Km* reflects how well enzyme and substrate interacts, this increase in *K*m after immobilization indicates that the post-immobilization interaction between phytase and phytic acid is reduced. This reduced enzyme-substrate interacation is most likely due to the decrease in the free movement of phytase on the solid AuNPs^{Tyr} support, either due to the steric hindrance of the active site of phytase by AuNPs^{Tyr} or due to the compromise of enzymatic flexibility necessary for substrate binding or a combination of both, thereby leading to the mass transfer resistance of the substrate into the immobilization medium (AuNPs^{Tyr}/Phytase).[41] Similarly, *Vmax* of native and immobilized enzyme varied with temperature, with *Vmax* values of 14956.92 and 18171.28 M/sec obtained for native phytase and AuNPs^{Tyr}/Phytase,

respectively, at the optimum temperature of 55 °C. While *Km* provides an indication of the strength of enzyme-substrate interaction, *Kcat* indicates how fast the enzyme works, and therefore, the specificity constant *Kcat*/*Km* provides an indication on the specificity of an enzyme towards a particular substrate. At 55 °C, *Kcat*/*Km* of native and immobilized phytase were 49.47 x 10^5 and 17.77 x 10^5 $M^{-1}sec^{-1}$, respectively, which shows that while the native phytase may show high specificity towards phytic acid, the immobilized phytase might also be able to act non-specifically on similar substrates. Although the substrate specificity of enzymes is typically considered a desirable characteristic, in context of phytase that has application in release of inorganic phosphorous from a variety of animal feedstock, the ability of $AuNPs^{Tyr}$/Phytase to act on a variety of substrates is certainly more desirable.

Another important indication of enzymatic efficiency can be obtained by calculating the energy of activation (*Ea*) of an enzyme from the slope of the Arrhenius plot of ln *Vmax* versus 1/*T* (**Figure 4**). It was interesting to observe that the *Ea* of phytic acid hydrolysis of immobilized phytase (35001.94 J/M) was 1.5 times lower than that of native phytase (53001.75 J/M), indicating that the reaction is kinetically controlled. The significant reduction in the *Ea* in $AuNPs^{Tyr}$/Phytase indicates that the enzyme immobilization has the capability to improve the overall quality of phytase by lowering down the energy barrier required to achieve the transition state activated complex, thereby allowing the enzymatic reaction to occur with a faster rate.[37] It is also notable from Figure 4 that the native phytase has a steeper slope in comparison with the immobilized phytase, indicating that after immobilization of phytase on $AuNPs^{Tyr}$, the enzyme activity has lower sensitivity to the change in temperature. This aspect has important implications for the use of AuNPs/Phytase for commercial applications, as enzymes that are operational at wider temperature ranges are preferred.

Gibbs free energy (ΔG^*) of native phytase at 55 °C was -19609.60 J/M, which changed to -16284.50 J/M after its immobilization, indicating that the driving force for reaction of AuNPs^{Tyr}/Phytase nanozyme composite was decreased than the native phytase. The ΔG of native phytase decreased with the increase in temperature up to 50 °C and then increased further above it, however, for AuNPs^{Tyr}/Phytase, it was decreased with increase in temperature upto 55 °C and increased further at 60 °C. Further, the enthalpy of activation of thermal unfolding (ΔH^*) of native and immobilized phytase at 55 °C were 50273.51 and 32273.70 J/M, respectively, which remained constant throughout the tested temperature range. However, the thermostability of AuNPs^{Tyr}/Phytase nanozyme composite is accompanied by reduced ΔH^* values, which suggests that during immobilization, the conformation of phytase is altered in such a manner that it either leads to the reduction in the hydrophobic core of the immobilized phytase or the immobilized enzyme achieves a partially unfolded transition state or a combination of both. This is because thermal denaturation of proteins is typically accompanied by the disruption of non-covalent interactions such as hydrophobic interactions, which typically results in an increase in the enthalpy of activation.[37] Entropy (ΔS) has a positive sign, that suggesting entropy-driven association process. More precisely, since the signs for enthalpy and entropy are positive, it can be said that the process is spontaneous at high temperatures, and the exothermicity of the process has a small role in reaction balance. However, thermodynamics of AuNPs^{Tyr}/Phytase nanozyme composite showed the decrease in enthalpy and entropy values compared to native phytase. This might be owing to the fact that with the increase in particle's hydrodynamic diameter after phytase immobilization, entropy decreases and this might lead to decreased potential between phytase and AuNPs^{Tyr} surface.[42]

Considering that AuNPs^{Tyr}/Phytase nanozyme composite improves the thermostability of this enzyme, it was further tested for reusability studies up to 10 enzymatic cycles (**Figure 5**). A gradual decrease in the enzymatic activity, leading to 60% residual activity after 10th cycle was observed. Since no sharp decline in residual activity was observed, the observed activity loss is most likely due to the incomplete recovery of phytase from the reaction vessel during centrifugation-mediated precipitation and washing steps.

4. Conclusions

This study demonstrates the important role that a charge-switchable reducing/capping agent may play toward controlling metal nanoparticle surface corona for biological applications. This has been demonstrated in the current case by employing zwitterionic tyrosine amino acid as a reducing and capping agent for the synthesis of gold nanoparticles. The surface of these tyrosine-capped gold nanoparticles could be efficiently biofunctionalized with phytase enzyme in a facile manner by controlling the pH of the reaction while considering the isoelectric points of tyrosine and phytase. The pH-dependent charge-switchable nature of tyrosine allowed spontaneous immobilization of phytase on the gold nanoparticle surface through electrostatic interactions. The immobilized phytase showed an overall improved performance over native phytase by lowering the energy of activation required for the product formation, increasing the enzyme thermostability, expanding the operating temperature window in which immobilized phytase could operate, and enabling phytase reusability over multiple cycles. We recently demonstrated that a similar amino acid-based charge-switching strategy could be employed to develop antimicrobial nanomaterials that were specifically active against bacteria without causing toxicity to mammalian cells.[23] We also demonstrated the importance of such charge-switching molecules in SERS-based sensing of analyte molecules.[26] The current study along with our

recent efforts in this area strongly suggest that the significant variability in the isoelectric points and the hydropathy indices of 20 natural amino acids and the characteristic charge-switchability feature of these simple biological building blocks is likely to offer unique opportunities at the nano-bio interface. Aforementioned features of zwitterionic amino acids along with the ability of some of the amino acids (e.g. tyrosine, tryptophan and proline) to reduce metal ions will be attractive for controlling metal nanoparticle surface corona for a variety of biological applications.

Acknowledgements

S. Shankar duly acknowledges Department of Education, Commonwealth of Australia for Endeavour Research Award. H.K Daima acknowledges Government of India, New Delhi (India) for National Overseas Scholarship. V. Bansal acknowledges the Australian Research Council (ARC) for a Future Fellowship (FT140101285) and research support through the ARC Linkage (LP130100437) scheme. VB also acknowledges the generous support of the Ian Potter Foundation for establishing an Ian Potter NanoBioSensing Facility at RMIT University. Authors acknowledge the support of RMIT node of Australian Microscopy and Microanalysis Research Facility (AMMRF) for providing technical assistance and access to their characterization facilities.

References

[1] N. R. Reddy, S.K. Sathe and D.K. Salunkhe, *Adv. Food Res*., 1982, **28,** 1–92.

[2] E. J. Mullaney, C. B. Daly and A. H. J. Ullah, Adv. Appl. *Microbiol*., 2000, **47**, 157–199.

[3] K. Bhavsar, P. Gujar, P. Shah, V. R. Kumar and J. M. Khire, *Appl. Microbiol. Biotechnol*., 2013, **97**, 673–679.

[4] V. Kumar, D. Singh, P. Sangwan and P. K. Gill, in *Applied Environmental Biotechnology: Present Scenario and Future Trends,*ed. G. Kausik , Springer, India, 2015, ch 7, pp 97–114 .

[5] T. Nuge, Y. Z. H. Y. Hashim, A. E. A. Farouk and H. M. Salleh, *Advances in Enzyme Research*, 2014, **2**, 27–38.

[6] A. Vohra and T. Satyanarayana, *Process Biochem*., 2002, **37**, 999–1004.

[7] E. J. Mullaney and A. H. J. Ullah, *Biochem. Bioph. Res. Co*., 2005, **328**, 404–408.

[8] C.Ó. Fágáin, *Enzyme Microb. Technol*., 2003, **33**, 137–149.

[9] T. K. Sharma, R. Ramanathan, R. Rakwal, G. K. Agarwal and V. Bansal, *Proteomics.*, 2015, **15**, 1680-1692.

[10] G. K. Agarwal, A. M. Timperio, L. Zolla, V. Bansal, R. Shukla and R. Rakwal, *J. Proteomics*., 2013, **93**, 74-92.

[11] A. Tanksale, P. M. Chandra, M. Rao and V Deshpande, *Biotechnol. Lett*., 2001, **23**, 51–54.

[12] S. Shankar and R. S. Laxman, *Environmental Engineering and Management Journal*., 2010, **10**, 1727–1732.

[13] B. L. Liu, C. H. Jong and Y. M. Tzeng, *Enzyme Microb. Technol*., 1999, **25**, 517–521.

[14] D. Menezes-Blackburn, M. Jorquera, L. Gianfred, M. Rao, R. Greiner, E. Garrido and M. L. Mor, *Bioresour. Technol*., 2011, **102**, 9360–9367.

[15] E. A. Cho, E. J. Kim and J. G. Pan, *Enzyme Microb. Technol*., 2011, **49**, 66–71.

[16] L. Mosafa, M. Moghadam and M. Shahedi, *Chinese J. Catal*., 2013, **34**, 1897–1904.

[17] S. K. Soni, R. Ramanathan, P. J. Coloe, V. Bansal and S. K. Bhargava, *Langmuir*., 2010, **26**, 16020–16024.

[18] S. K. Soni, P. R. Selvakannan, S. K. Bhargava and V Bansal , *Langmuir*., 2012, **28**, 10389–10397.

[19] A. Gole, C. Dash, V. Ramakrishnan, S. R. Sainkar, A. B. Mandale, M. Rao and M. Sastry, *Langmuir*., 2001, **17**, 1674–1679.

[20] A. Gole, S. Vyas, S. Phadtare, A. Lachke and M. Sastry, *Colloid. Surf. B.*, 2002, **25**, 129–138.

[21] J. Xu, J. Sun, Y. Wang, J. Sheng, F. Wang and M. Sun, *Molecules*., 2014, **19**, 11465–11486.

[22] H. K. Daima, P. R. Selvakannan, R. Shukla, S. K. Bhargava and V. Bansal, *PLoS ONE*., 2013, **8,** e79676.

[23] H. K. Daima, P. R. Selvakannan, A. E. Kandjani, R. Shukla, S. K. Bhargava and V Bansal, *Nanoscale*., 2014, **6**., 758–765.

[24] P. Weerathunge, R. Ramanathan, R. Shukla, T. K. Sharma and V. Bansal, *Anal. Chem.*, 2014, **86**, 11937–11941.

[25] T. K. Sharma, R. Ramanathan, P. Weerathunge, M. Mohammadtaheri, H. K. Daima, R. Shukla and V. Bansal, *Chem. Comm.*, 2014, **50**, 15856–15859.

[26] P. R. Selvakannan, R. Ramanathan, B. J. Plowman, Y. M. Sabri, H. K. Daima, A. P. O'Mullane, V. Bansal and S. K. Bhargava, *Phys. Chem. Chem. Phys.*, 2013, **15**, 12920–12929.

[27] R. Shukla , V. Bansal , M. Chaudhary, A. Basu , R.R. Bhonde and M. Sastry, *Langmuir*., 2005, **21**, 10644–10654.

[28] S. K. Soni and J. M. Khire, *World J. Microbiol. Biotechnol*., 2007, **23**, 1585–1593.

[29] T. N. Mandviwala and J. M. Khire, *J. Ind. Microbiol. Biotechnol*., 2000, **24**, 237–243.

[30] J. K. Heinonen and R. J. Lahti, *Anal. Biochem*., 1981, **113**, 313–317.

[31] M. M. Bradford, *Anal. Biochem*., 1976, **72**, 248–254.

[32] K. S. Shashidhara and S. M. Gaikwad, *Int. J. Biol. Macromol*., 2009, **44**, 112–115.

[33] S. Shankar and R. S. Laxman, *Appl. Biochem. Biotechnol*., 2015, **175**, 589–602.

[34] S. K. Soni, A. S. Magadum and J. M. Khire, *World J. Microbiol. Biotechnol*., 2010, **26**, 2009–2018.

[35] H. J. Ullah, B. J. Cummins and H. C. Dischinger, *Biochem. . Bioph. Res. Co.*, 1991, **178**, 45–53.

[36] J. F. Hainfeld, W. Liu, C. M. R. Halsey, P. Freimuth and R. D. Powell, *J. Struct. Biol*., 1999, **127**, 185–198.

[37] R. S. Singh, G. K. Saini and J. F. Kennedy, *Carbohydr. Polym*., 2010, **81**, 252–259.

[38] A. M. Fayaz , M. Girilal, M. Rahman, R. Venkatesan and P. T. Kalaichelvan, *Process Biochem*., 2011, **46**, 1958–1962.

[39] M. Alauddin, K. K. Kim, M. Roy, J. K. Song, M. S. Kim and S. M. Park, *Bull. Korean Chem. Soc.*, 2013, **34**, 188–196.

[40] B. Hu, J. Pan, H. L. Yu, J. W. Liu and J. H. Xu, *Proc. Biochem.*, 2009, **44**, 1019-1024.

[41] M. Y. Chang and R. S. Juang, *Enz. Microb. Technol*., 2005, 36, 75-82.

[42] G. A. Barhate, S. M. Gaikwad, S. S. Jadhav and V. B. Pokharkar, *Int. J. Pharm.*, 2014, **471**, 439–448.

Temp (C)	*Vmax* (M phosphorus release/M phytase/sec)		*Km* (M)		*Kcat* (/sec)		*Kcat/Km* (/M/Sec)		ΔG* Phy (J/M)		ΔH* (J/M)		ΔS* (J/M/K)	
	Phy	Au/Phy	Phy	Au/Phy	Phy	Au/Phy	Phy	Au/Phy	Phy	Au/Phy	Phy	Au/Phy	Phy	Au/Phy
35	7134.19	7705.47	0.53×10^{-3}	0.68×10^{-3}	1783.55	1926.37	33.72×10^{5}	28.24×10^{5}	-19329.4	-18677.61	50439.79	32439.98	226.41	165.88
40	10076.07	9019.74	0.56×10^{-3}	0.85×10^{-3}	2519.02	2254.93	44.62×10^{5}	26.56×10^{5}	-19473.0	-18411.01	50398.22	32398.41	223.12	162.25
50	17788.40	13069.74	1.31×10^{-3}	1.71×10^{-3}	4447.10	3267.44	33.92×10^{5}	19.12×10^{5}	-17831.4	-17119.29	50315.08	32315.27	210.88	152.98
55	14956.92	18171.28	0.76×10^{-3}	2.56×10^{-3}	3739.23	4542.82	49.47×10^{5}	17.77×10^{5}	-19609.6	-16284.54	50273.51	32273.70	212.96	147.98
60	13486.60	13068.97	1.14×10^{-3}	1.03×10^{-3}	3371.65	3267.24	29.52×10^{5}	31.60×10^{5}	-18764.8	-19040.99	50231.94	32232.13	207.10	153.90

Phy = native phytase; Au/Phy = $AuNPs^{Tyr}$/Phytase nanozyme composite; *Vmax* = maximum velocity; *Km* = Michaelis constant; *Kcat* = first order rate constant; ΔG* = Gibbs free energy; ΔH* = enthalpy of activation; and ΔS*=entropy of reaction.

Table 1. Substrate kinetic and thermodynamic parameters of native phytase and $AuNPs^{Tyr}$/Phytase nanozyme composite as a function of temperature.

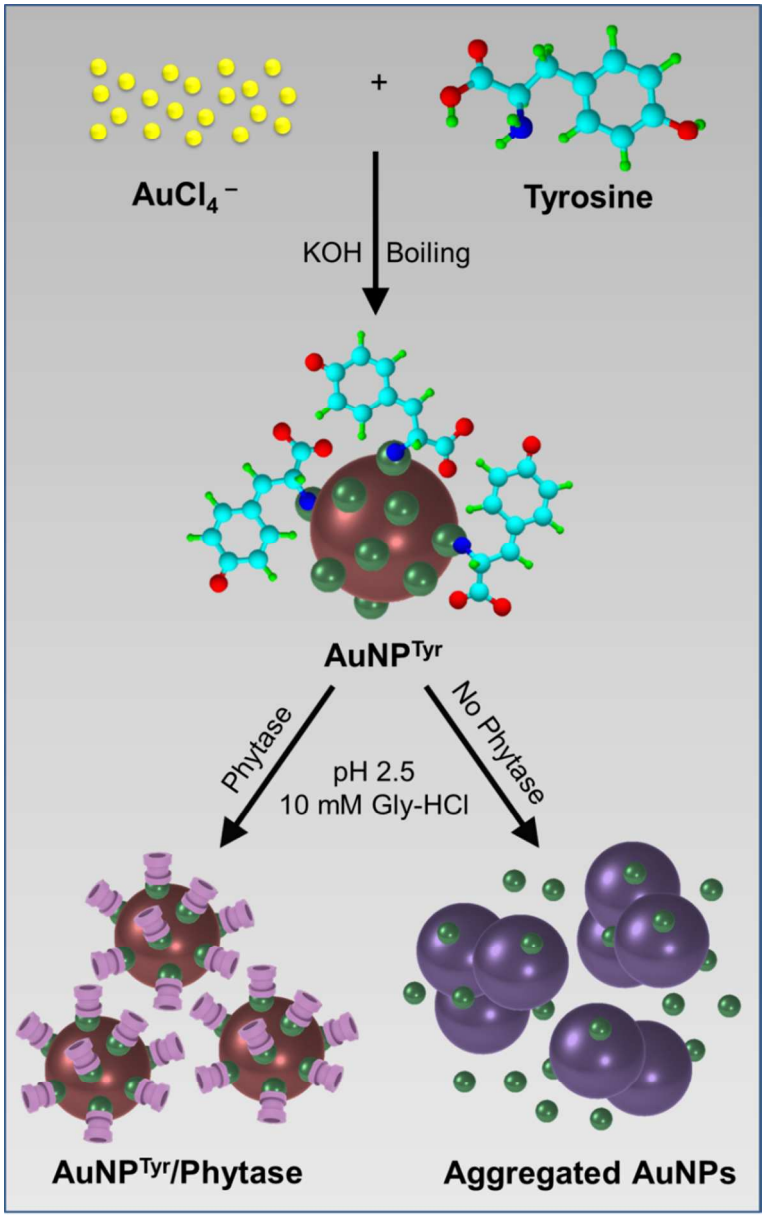

Scheme 1. Schematic representation of tyrosine-mediated synthesis of $AuNPs^{Tyr}$ and their biofunctionalization with phytase to form stable $AuNPs^{Tyr}$/Phytase. In tyrosine structure, cyan, red, blue and green represent C, O, N and H atoms, respectively. The green balls on the surface of gold nanoparticles represent oxidized tyrosine molecules, whereas the magenta structures represent phytase enzyme. The oxidation of phenol group in tyrosine molecules bound onto the surface of $AuNP^{Tyr}$ after reduction of $AuCl_4^-$ ions is notable.

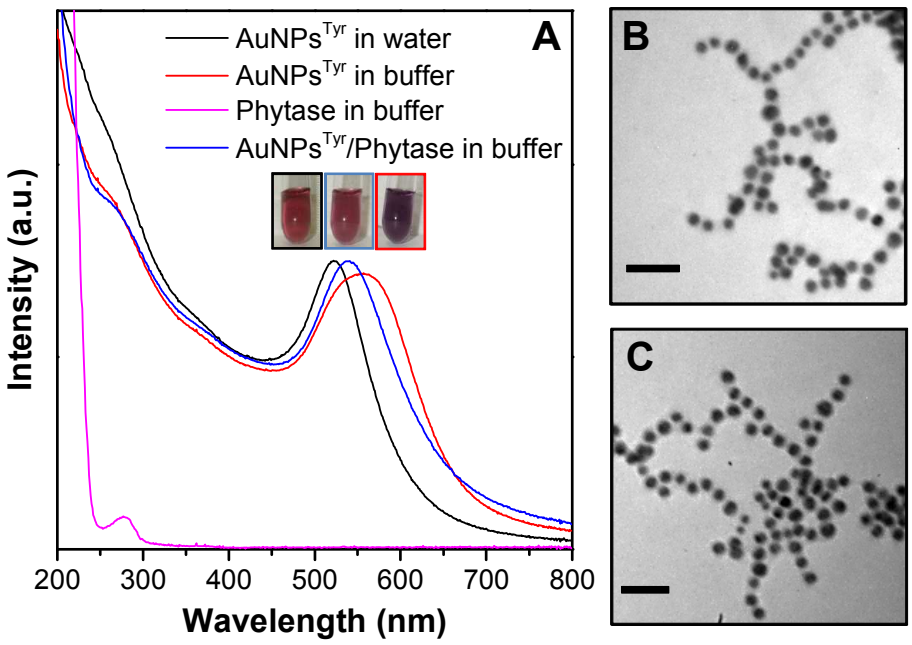

Fig. 1. (A) UV-Visible spectra of native phytase and gold nanoparticles at different stages of phytase immobilization, and (B-C) TEM images of (B) AuNPs^{Tyr} in water and (C) AuNPs^{Tyr}/Phytase in buffer. Scale bars correspond to 50 nm.

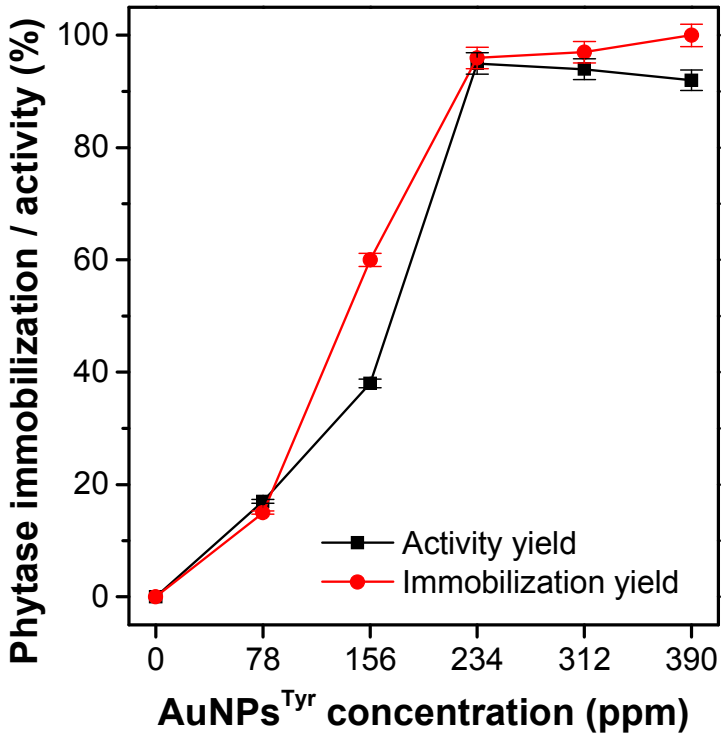

Fig. 2. Immobilization and activity yields of phytase as a function of gold concentration in $AuNPs^{Tyr}$.

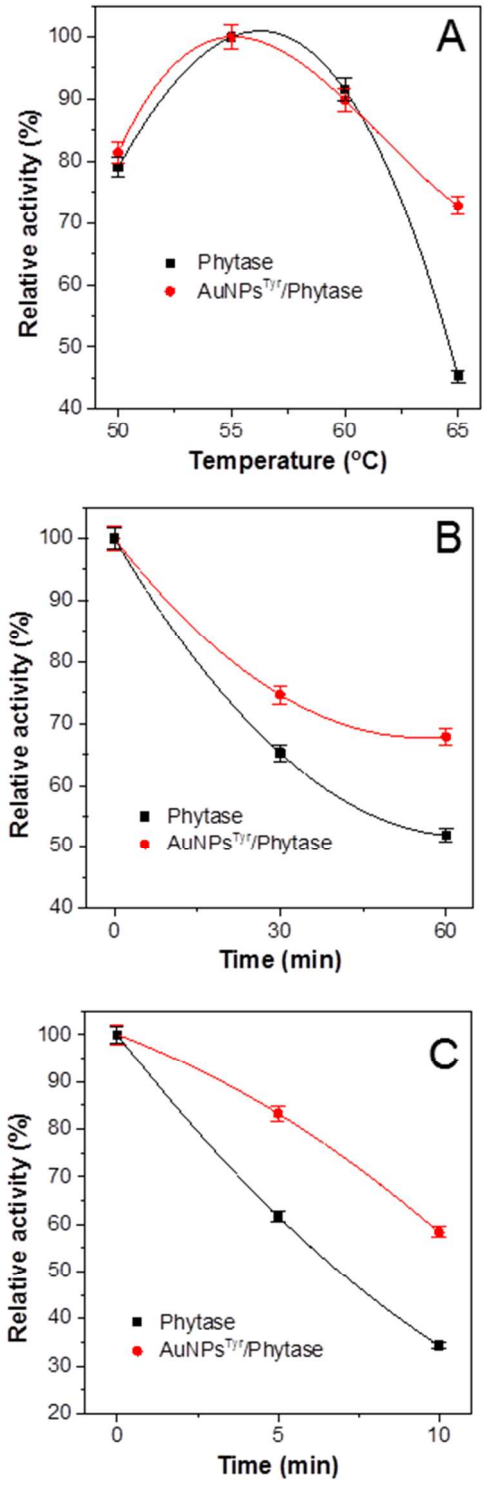

Fig. 3. Comparison of the thermostability of native phytase and AuNPs^{Tyr}/Phytase nanozyme composite (A) as a function of temperature, (B) as a fuction of time at 65 °C, and (C) as a fuction of time at 70 °C.

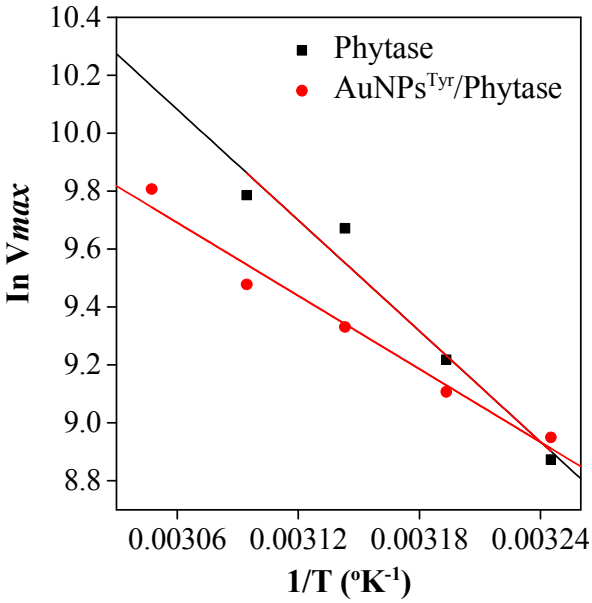

Fig. 4. Arrhenius plots for native phytase and AuNPs^{Tyr}/Phytase nanozyme composite to evaluate activation energies of the native and immobilized enzymes.

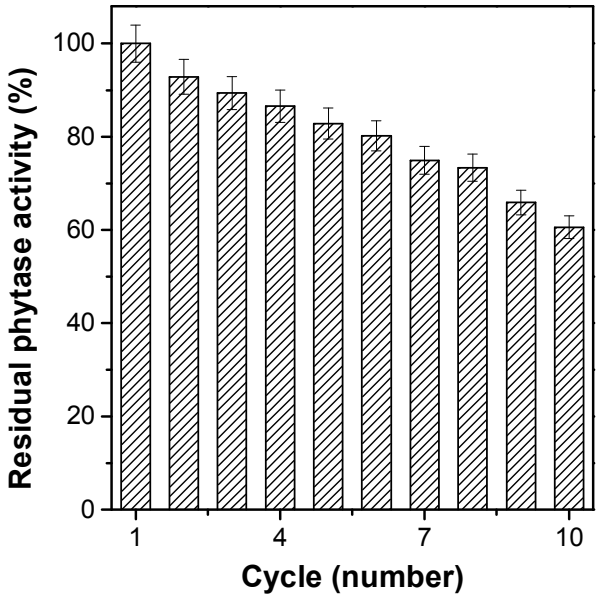

Fig. 5. Reusability study of AuNPs^{Tyr}/Phytase nanozyme composite for the hydrolysis of phytic acid.